

Effects of Catalyst Introduction Methods Using PAMAM Dendrimers on Selective Electroless Nickel Deposition on Polyelectrolyte Multilayers

Troy R. Hendricks, Erin E. Dams, Steven T. Wensing, and Ilsoon Lee*

Michigan State University, Department of Chemical Engineering and Materials Science, 2527 Engineering Building, East Lansing, Michigan 48824

Received March 12, 2007. In Final Form: April 16, 2007

We studied the effects of catalyst introduction methods using poly(amidoamine) (PAMAM) dendrimers on the nickel patterning of polyelectrolyte multilayer (PEM)-coated substrates. Three different approaches to palladium catalyst introduction using microcontact printing as the patterning technique were utilized and compared. The catalyst introduction methods are (1) direct catalyst stamping, (2) directed assembly using PAMAM dendrimer stamping, and (3) catalyst encapsulation and reduction to nanoparticles within PAMAM dendrimers before stamping. After patterning, the sample surfaces were placed in an electroless bath where nickel was selectively plated onto the patterns. The patterned surfaces were characterized using optical microscopy, atomic force microscopy, scanning electron microscopy, and energy-dispersive X-ray spectroscopy. The metal plating rates on different homogeneous surfaces that simulate the patterned surfaces were measured using a quartz crystal microbalance. In addition, the effect of PEM film thickness (i.e., number of bilayers) on the selectivity of nickel patterning was investigated.

Introduction

A new direction for research in thin-film transistors, organic light-emitting diodes, and other microelectronic devices is to find methods that will enable the fabrication of flexible devices.^{1,2} Recently, we showed that the combination of polyelectrolyte multilayer (PEM) coatings, microcontact printing (μ CP), and electroless deposition (ELD) can be used to create metal patterns on a variety of different substrates.³ The layer-by-layer (LbL) assembly of polyelectrolytes is an inexpensive method of creating a surface with properties that are independent from those of the substrate.⁴ The different types of substrates include glass, metal oxides, silicon wafers, and both stiff and flexible plastics. μ CP is a simple soft lithographic approach to patterning that uses an elastomeric stamp to create patterns over large surface areas.⁵ This method is more advantageous than the current technique, photolithography, because it allows for the use of nonplanar substrates and does not severely limit the types of materials that can be used. ELD is a nanoscale metal deposition technique that can selectively pattern 3D surfaces.^{6,7}

μ CP and ELD have been combined to fabricate patterns of various types of metals.^{8–13} Silane self-assembled monolayers,

titanium, and polymers have been used as adhesion layers with which to attach the ELD catalysts to their substrates. However, all of these approaches use specific interactions between the adhesion layer and the substrate that are not universal like electrostatic charges. If the substrate is changed, then these other methods are ineffective; however, using a PEM adhesion layer allows for a variety of substrates to be used.^{3,14,15}

Cagelike poly(amidoamine) (PAMAM) dendrimers that offer precise control of their nanoscale size have been patterned using μ CP.^{16–18} These dendrimers are more advantageous for patterning because they do not diffuse on the surface like lower-molecular-weight materials such as alkane thiols. The hollow dendrimer interiors can be used to store functional nanomaterials. Crooks and co-workers have shown that nearly monodisperse nanoparticles can be created inside the PAMAM dendrimers.¹⁹ The interiors of the dendrimers serve as binding groups for metal ions. Once the ions are encapsulated, they are reduced to form nanoparticles. These nanoparticles can be used as catalysts for hydrogenation and other types of reactions. Additionally, Bittner and co-workers have created micropatterns of PAMAM dendrimers and utilized them as adhesion layers for ELD.^{20,21} Most ELD papers show how to create metal patterns; no research has investigated how different methods of introducing the catalyst to a surface affect the resulting metal patterns.

In this work, we show for the first time how the method of catalyst introduction affects the resulting patterned electroless

* Corresponding author. E-mail: leeil@egr.msu.edu. Phone: (517) 355-9291. Fax: (517) 432-1105.

(1) Khang, D. Y.; Jiang, H. Q.; Huang, Y.; Rogers, J. A. *Science* **2006**, *311*, 208–212.

(2) Zhang, D. H.; Ryu, K.; Liu, X. L.; Polikarpov, E.; Ly, J.; Tompson, M. E.; Zhou, C. W. *Nano Lett.* **2006**, *6*, 1880–1886.

(3) Hendricks, T. R.; Lee, I. *Thin Solid Films* **2006**, *515*, 2347–2352.

(4) Decher, G. *Science* **1997**, *277*, 1232–1237.

(5) Geissler, M.; Xia, Y. N. *Adv. Mater.* **2004**, *16*, 1249–1269.

(6) Lee, I.; Hammond, P. T.; Rubner, M. F. *Chem. Mater.* **2003**, *15*, 4583–4589.

(7) Radloff, C.; Vaia, R. A.; Brunton, J.; Bouwer, G. T.; Ward, V. K. *Nano Lett.* **2005**, *5*, 1187–1191.

(8) Tjong, V.; Wu, L.; Moran, P. M. *Langmuir* **2006**, *22*, 2430–2432.

(9) Carmichael, T. B.; Vella, S. J.; Afzali, A. *Langmuir* **2004**, *20*, 5593–5598.

(10) Geissler, M.; Kind, H.; Schmidt-Winkel, P.; Michel, B.; Delamarche, E. *Langmuir* **2003**, *19*, 6283–6296.

(11) Hidber, P. C.; Helbig, W.; Kim, E.; Whitesides, G. M. *Langmuir* **1996**, *12*, 1375–1380.

(12) Kind, H.; Geissler, M.; Schmid, H.; Michel, B.; Kern, K.; Delamarche, E. *Langmuir* **2000**, *16*, 6367–6373.

(13) Kohli, N.; Hassler, B. L.; Parthasarathy, L.; Richardson, R. J.; Ofoli, R. Y.; Worden, R. M.; Lee, I. *Biomacromolecules* **2006**, *7*, 3327–3335.

(14) Guo, T. F.; Chang, S. C.; Pyo, S.; Yang, Y. *Langmuir* **2002**, *18*, 8142–8147.

(15) Wang, T. C.; Chen, B.; Rubner, M. F.; Cohen, R. E. *Langmuir* **2001**, *17*, 6610–6615.

(16) Arrington, D.; Curry, M.; Street, S. C. *Langmuir* **2002**, *18*, 7788–7791.

(17) Li, H. W.; Kang, D. J.; Blamire, M. G.; Huck, W. T. S. *Nano Lett.* **2002**, *2*, 347–349.

(18) Kohli, N.; Dvornic, P. R.; Kaganove, S. N.; Worden, R. M.; Lee, I. *Macromol. Rapid Commun.* **2004**, *25*, 935–941.

(19) Scott, R. W. J.; Wilson, O. M.; Crooks, R. M. *J. Phys. Chem. B* **2005**, *109*, 692–704.

(20) Bittner, A. M.; Wu, X. C.; Kern, K. *Adv. Funct. Mater.* **2002**, *12*, 432–436.

(21) Wu, X. C.; Bittner, A. M.; Kern, K. *Langmuir* **2002**, *18*, 4984–4988.

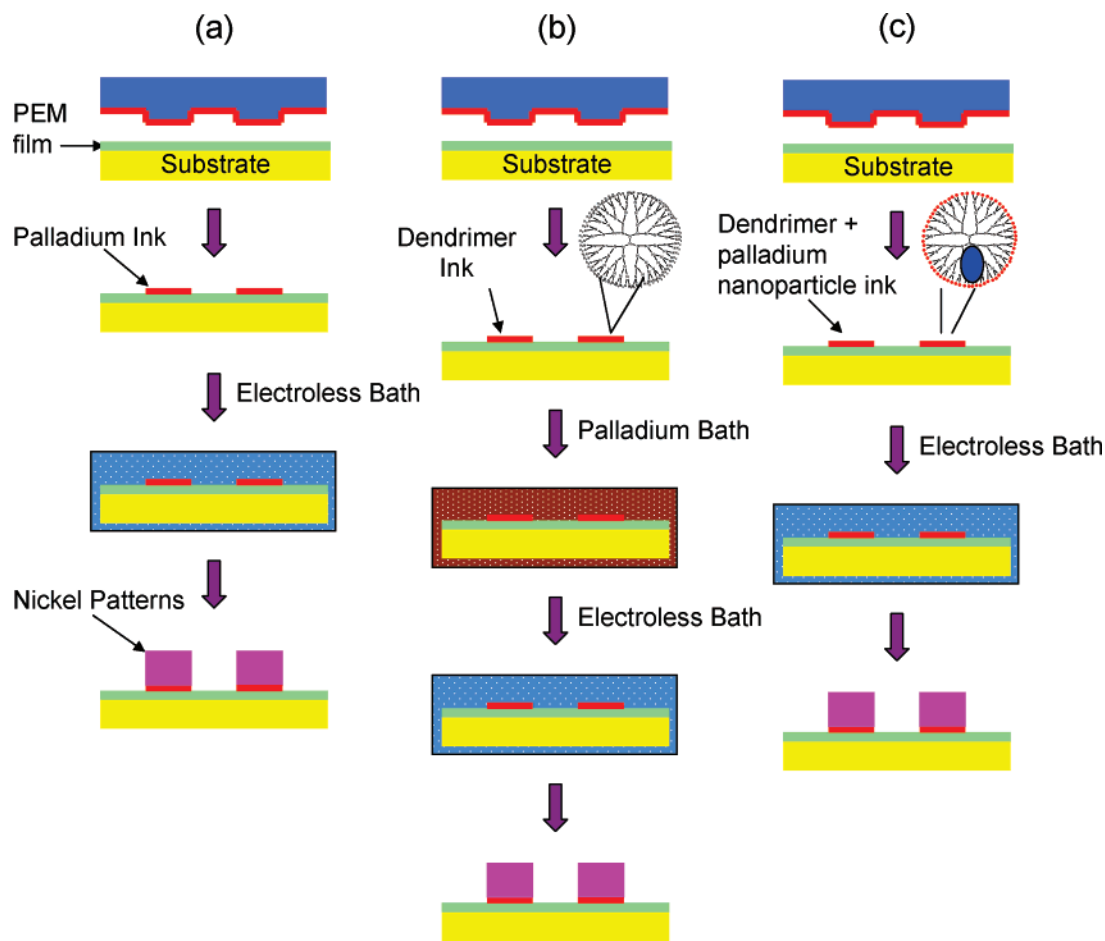


Figure 1. Process schematic for the three different methods. Methods 1–3 are depicted in parts a–c, respectively. Diagrams of the dendrimer and dendrimer-encapsulated nanoparticle structures are also included in parts b and c, respectively.

Table 1. Summary of the Three Different Catalyst Introduction Methods

	name	PEM outer surface	ink	additional steps
method 1	direct catalyst stamping	PDAC	Pd catalyst	none
method 2	directed assembly	SPS	G4 dendrimer	adsorb Pd ions
method 3	dendrimer assembly	SPS	Pd in G4 dendrimer	none

deposition. PEM films were fabricated and used as platforms for electroless nickel patterning. μ CP was used to pattern the palladium catalyst on the PEM platforms. After applying the catalyst, the samples were placed into an electroless bath. In the electroless bath, the initial nickel plating rate, nickel morphology, and nickel pattern selectivity (i.e., relative amount of metal deposition in desired places versus undesired places) were all affected by the method of catalyst introduction. Also, the number of PEM bilayers required to remove the substrate effect on nickel patterning was investigated.

Materials and Methods

Materials. Poly(diallyldimethylammonium chloride) (PDAC, $M_w \sim 70\,000$), sulfonated poly(styrene), sodium salt (SPS, $M_w \sim 150\,000$), fourth generation poly(amidoamine) (G4 PAMAM) dendrimers, nickel sulfate, sodium citrate, lactic acid, dimethylamine borane (DMAB), and 16-mercaptohexadecanoic acid were purchased from Sigma-Aldrich (Milwaukee, WI). The palladium catalyst, $\text{Na}_2[\text{PdCl}_4]$, was purchased from Strem Chemicals (Newburyport, MA). A Sylgard 184 elastomer kit was obtained from Dow Corning (Midland, MI) to create poly(dimethylsiloxane) (PDMS) stamps. Fluorescein isothiocyanate (FITC) was purchased from Molecular Probes (Eugene, Oregon). Deionized (DI) water from a Barnstead Nanopure Diamond (Barnstead International, Dubuque, IA, resistivity $> 18.2\ \text{M}\Omega\cdot\text{cm}$) purification system was used exclusively for all experiments.

Substrate Preparation. A Branson ultrasonic cleaner (Branson Ultrasonics Corporation, Danbury, CT) was used to sonicate glass microscope slides for 20 min with an aqueous Alconox (Alconox Inc., New York, NY) solution and again for 10 min in water alone. Slides were then dried under a stream of nitrogen and were further cleaned with oxygen plasma treatment in a Harrick Plasma cleaner (Harrick Scientific Corporation, Broadway Ossining, New York) for 10 min at a pressure of ~ 0.125 Torr. PEMs of positively charged PDAC and negatively charged SPS were deposited onto the microscope slides using a computer-controlled mechanical Carl Zeiss slide stainer (Richard-Allan Scientific, Kalamazoo, MI). Both polyelectrolyte concentrations were 0.02 M (based on the polymer repeat unit) and contained 0.1 M NaCl. One layer of PDAC followed by a layer of SPS was used to create a single bilayer. A PDAC-topped 10.5 bilayer film, denoted as $(\text{PDAC}/\text{SPS})_{10.5}$, was used when a positive surface was desired. A SPS-topped 10 bilayer film, denoted as $(\text{PDAC}/\text{SPS})_{10}$, was used when a negative surface was desired.

Stamp Preparation. Patterned silicon masters were obtained from the Keck Microfabrication Facility at Michigan State University. The patterns consisted of circular patterns with diameters ranging from 1.25 to 9.0 μm . PDMS stamps were fabricated by mixing the prepolymer and initiator (10:1) and pouring the mixture onto the patterned silicon master. The stamps were then cured overnight in an oven at 60 $^\circ\text{C}$. Before use, the stamps were oxygen plasma treated for 30 s to render the surface hydrophilic. A cotton-tipped swab was used to apply different inks to the stamp surface before drying with

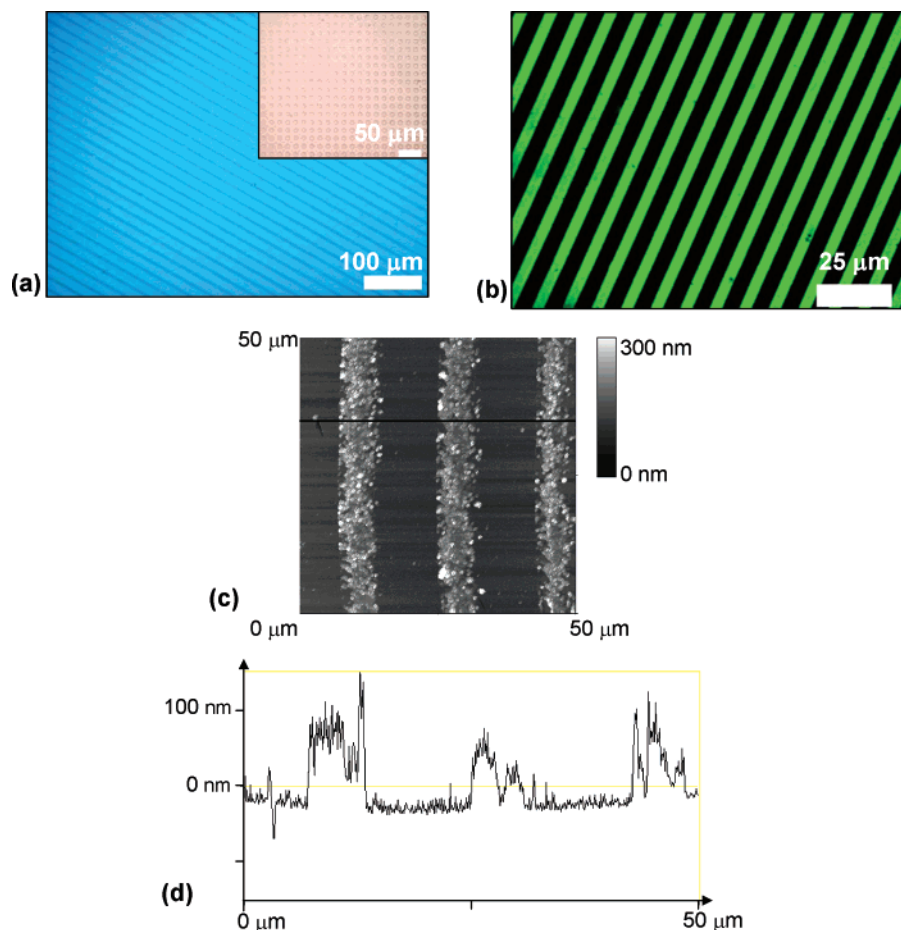


Figure 2. Optical microscope and AFM images of G4 PAMAM dendrimer patterns on PEMs. (a) Phase contrast optical microscope images of two different pattern types with (large) and without (inset) a blue filter, (b) fluorescent microscope image of FITC-labeled PAMAM, (c) topographical AFM image of PAMAM patterns, and (d) sample line scan taken from the AFM image shown in c.

nitrogen. The contact time with the appropriately charged surfaces was typically 20 s.

Ink Preparation. Three different methods were used to introduce the palladium catalyst to PEM surfaces: direct catalyst stamping (method 1), directed assembly (DA, method 2) using PAMAM dendrimers, and catalyst encapsulation (method 3) and reduction to nanoparticles inside PAMAM dendrimers. These methods are summarized in Table 1. The inks used in each method were prepared as follows.

1. **Direct Catalyst Stamping.** A 50 mM solution of the palladium catalyst was directly stamped onto a PDAC surface and rinsed with pH \sim 3.0 water. Nitrogen was used to dry the samples.

2. **Directed Assembly.** A 0.1 wt % solution of G4 PAMAM in DI water was stamped onto an SPS surface. The substrate was immersed in a 5 mM palladium catalyst solution for 10 s and washed with DI water. The patterned substrates were then immersed in a 5 mM palladium catalyst solution for 10 s, and the substrate was then washed in pH \sim 3.0 water and dried with nitrogen.

PAMAM dendrimers were fluorescently labeled with FITC using a standard procedure.¹⁸ FITC was dissolved in water and then added to aqueous solutions containing PAMAM dendrimers using a 1:1 molecular ratio. The dendrimer and dye solution was allowed to stand overnight with light agitation and was then placed in dialysis tubing and dialyzed against DI water overnight.

3. **Catalyst Encapsulation.** The palladium catalyst ions were placed in the interiors of G4 PAMAM dendrimers and reduced to form dendrimer-encapsulated nanoparticles following a previously established protocol published by Crooks and co-workers.²² The pH of a 0.1 wt % G4 dendrimer solution in DI water was reduced to

\sim 3.0 using 0.1 M HCL. Then 563 μ L of 0.1 M $\text{Na}_2[\text{PdCl}_4]$ was slowly added to the dendrimer solution. This gives a dendrimer/Pd ion ratio of 1:40. The sample was allowed to mix for 30 min before adding a 10 molar excess (0.025 g) of DMAB to the solution, which reduces the Pd ions to metal nanoparticles. The solution was then filtered to remove large agglomerates.

Electroless Nickel Deposition. The catalyst-patterned slides were then placed in an electroless nickel bath. The nickel bath contained 4.0 g of nickel sulfate (Ni source), 2.0 g of sodium citrate (complexant), 1.0 g of lactic acid (buffer, complexant), and 0.2 g of DMAB (reducing agent) in 100 mL of DI water. Before use, the pH of the nickel bath was adjusted to 6.5 ± 0.1 by adding small amounts of a NaOH solution. Catalyzed substrates were placed into the electroless bath for plating times between 10 and 15 min.

Quartz Crystal Preparation. Gold-coated quartz crystals (5 MHz, Maxtek, Inc., Cypress, CA) were cleaned for 30 s in piranha solution (7:3 concd $\text{H}_2\text{SO}_4/30\% \text{H}_2\text{O}_2$). The crystals were immersed in an ethanol solution containing 5 mM 16-mercaptohexadecanoic acid for 20 min, followed by rinsing in copious amounts of ethanol. The negatively charged samples were then placed in the slide stainer where $(\text{PDAC}/\text{SPS})_{10}$ or $(\text{PDAC}/\text{SPS})_{10.5}$ bilayer films were assembled on their surfaces as described above. To simulate method 1, $(\text{PDAC}/\text{SPS})_{10.5}$ bilayer films were used. To simulate methods 2 and 3, $(\text{PDAC}/\text{SPS})_{10}$ bilayer films on quartz crystal microbalance (QCM) crystals were immersed in a 0.1 wt % G4 dendrimer solution for 20 min. For samples simulating method 3, the 0.1 wt % G4 solution contains dendrimer-encapsulated palladium nanoparticles. To activate the QCM crystals that simulated methods 1 and 2, the crystals were immersed for 10 s in an aqueous solution containing 5 mM palladium catalyst. The samples were then mounted in the crystal holder and placed into an electroless nickel bath. Computer

(22) Scott, R. W. J.; Ye, H. C.; Henriquez, R. R.; Crooks, R. M. *Chem. Mater.* **2003**, *15*, 3873–3878.

software was used to measure the change in the resonance frequency of the crystals.

Characterization. A Nikon Eclipse ME 600 microscope was used to obtain optical microscope images. A Nanoscope IV (Digital Instruments) multimode scope was used to obtain tapping mode AFM images. An Electro Scan scanning electron microscope (SEM, LaB₆ filament and 20 kV acceleration voltage) was used to obtain SEM images. A Link ISIS system (Oxford Instruments) was used to perform energy-dispersive X-ray spectroscopy (EDS). A research QCM (Maxtek, Inc.) and accompanying software were used to measure the nickel plating rates on different surfaces. A JEOL (Japanese Electro Optics Laboratories) 2200FS 200 kV field-emission transmission electron microscope (TEM) was used to obtain images of samples on carbon-coated copper grids.

Results and Discussion

Building on the combination of μ CP, ELD, and PEMs from our previous work,^{3,6} we explored different ways to introduce the catalyst to PEM surfaces. Using PAMAM dendrimers, we patterned the negatively charged palladium catalyst on the PEM surface using three different methods, as summarized in Table 1. Figure 1 illustrates the three different patterning methods that we utilized. After the catalyst is patterned on the surface, the samples are placed in an electroless nickel bath that exclusively plated nickel in the regions where palladium was present on the surface.

Figure 2 shows G4 PAMAM dendrimers patterned on SPS-coated PEM surfaces before further modification. Dendrimer patterns could be created to be as large as the stamp (~ 1 cm²). We used both ethanol and water as solvents in our ink solution. We found that either solvent can create excellent patterns but ethanol is easier to use because it evaporates faster than water. For nickel patterning in method 2, we used water as a solvent in the PAMAM ink so that all of the inks were water-based and could be directly compared. Using a 20 s contact time transferred multiple layers of dendrimers to the surface. Figure 2c shows that uniform patterns can be created before washing. The sample line scan in Figure 2d shows that the dendrimers have an average height of ~ 50 nm. This height of approximately 22 “monolayers” is consistent with thicknesses reported previously for μ CP G4 PAMAM on silicon wafers.¹⁶ After patterning, the samples were washed in water to remove the layer of weakly bound dendrimers and left only a strongly bound electrostatically bonded layer on the surface.²³ AFM shows that this strongly bound layer was typically 5–10 nm in thickness. The washed PAMAM surfaces were then used for nickel patterning.

To test method 3, palladium nanoparticles were created inside of the PAMAM dendrimers. The nanoparticle diameter was measured using TEM. Supporting Information shows a TEM image of the dendrimer-encapsulated nanoparticles and a graph of their size distribution. The dendrimers are not seen in the TEM image because they have little contrast against the carbon coating of the TEM grid. The average particle diameter was measured to be 1.6 ± 0.2 nm. This is consistent with previously reported values for nanoparticles created using a 40:1 ion/dendrimer ratio.^{22,24} These dendrimer-encapsulated nanoparticle solutions were then used as inks for electroless nickel patterning.

Oxygen-plasma-treated PDMS stamps were used to transfer the ink to the appropriately charged surface (Table 1). After patterning, samples were washed with DI water to remove excess ink that was not electrostatically bound to the surface. In method 2, after stamping, the samples were dipped into a 5 mM palladium

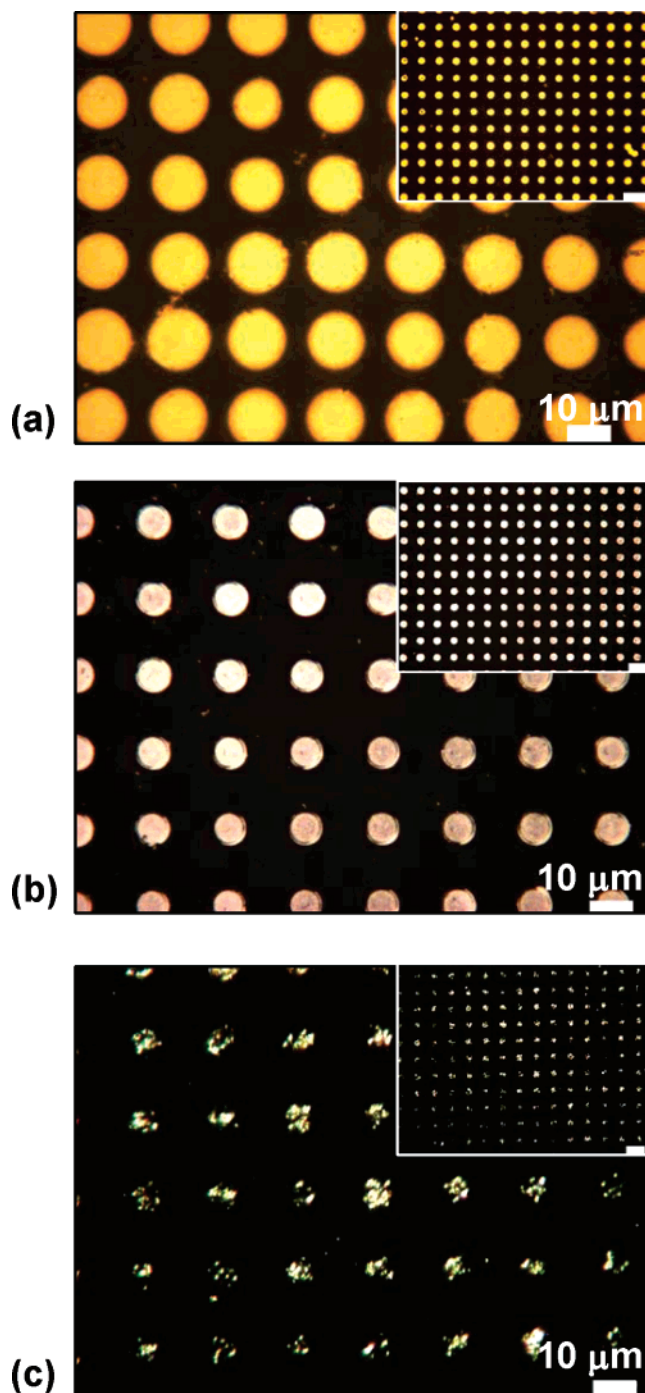


Figure 3. Optical microscope images of electroless-deposited nickel patterns. (a and b) Bright-field images of direct catalyst stamping (method 1) and DA (method 2) respectively. (c) Dark-field images of dendrimer-encapsulated nanoparticles (method 3). The insets show a larger sample area and have a 20 μ m scale bar.

solution, where the negatively charged palladium ions adsorbed onto the positively charged PAMAM dendrimers. For all three methods, after the catalyst was patterned, the samples were placed into an electroless nickel solution. In the ELD, bath nickel was selectively plated where the palladium catalyst was found on the surface. Figure 3 shows the resulting optical microscope images. All three methods successfully created nickel patterns on the PEM surfaces. The morphology of method 3 is noticeably different than the morphology observed in methods 1 and 2. This aggregated morphology of nickel was caused by the cage-like dendrimers that attached to the surface of the palladium nanoparticles and decreased the amount of active surface available for electroless

(23) Lee, I.; Ahn, J. S.; Hendricks, T. R.; Rubner, M. F.; Hammond, P. T. *Langmuir* **2004**, *20*, 2478–2483.

(24) Ye, H. C.; Scott, R. W. J.; Crooks, R. M. *Langmuir* **2004**, *20*, 2915–2920.

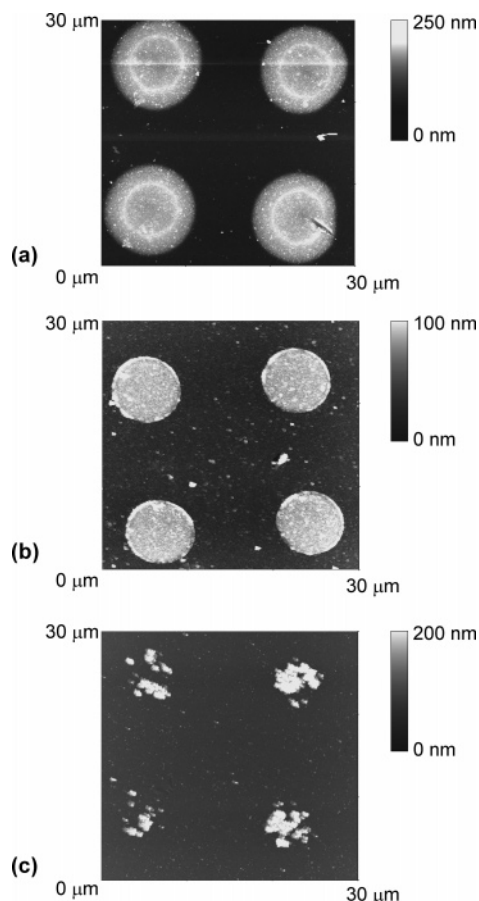


Figure 4. AFM images of nickel patterns using methods 1 (a), 2 (b), and 3 (c).

deposition. This smaller active surface prevented nickel ions in the electroless bath from depositing and being reduced on the palladium nanoparticle surface as rapidly as in methods 1 and 2. We also created samples that contained dendrimer-encapsulated palladium ions inside the dendrimers by leaving out the reduction step in ink preparation. These samples (Supporting Information image SI 2) show the same morphology as the dendrimer-encapsulated nanoparticles.

Figure 4 shows AFM images of the three different methods. Figure 4c, the AFM image for method 3, again shows the aggregated morphology caused by the encapsulation of the catalyst. A small number of exposed nanoparticles slowly grow in the electroless bath. As they become larger, they coalesce into one larger piece of nickel but still have the morphology of aggregated clusters. Method 1 had a higher selectivity than method 2. This is because in method 2 the DA of catalyst molecules onto the plus/minus micropatterned surfaces resulted in less selective nickel patterns. We believe that this occurred because the surface was not completely homogeneous. The inhomogeneous surface is created by the interpenetration between consecutive polyelectrolyte layers.⁴ This means that the multilayers are not exclusively plus or minus. Instead, there are small domains on the PEM surface where the tiny negatively charged catalyst molecules can find positively charged places on the unpatterned regions of an SPS surface. Only the direct catalyst stamping used in method 1 can create 100% selectivity. When comparing methods 2 and 3, we observed that the encapsulation of the catalyst into the interior of the dendrimer inhibited and confined the nickel deposition. To get the same pattern height as for the other two methods, dendrimer-encapsulated catalyst patterns required a longer time in the ELD bath.

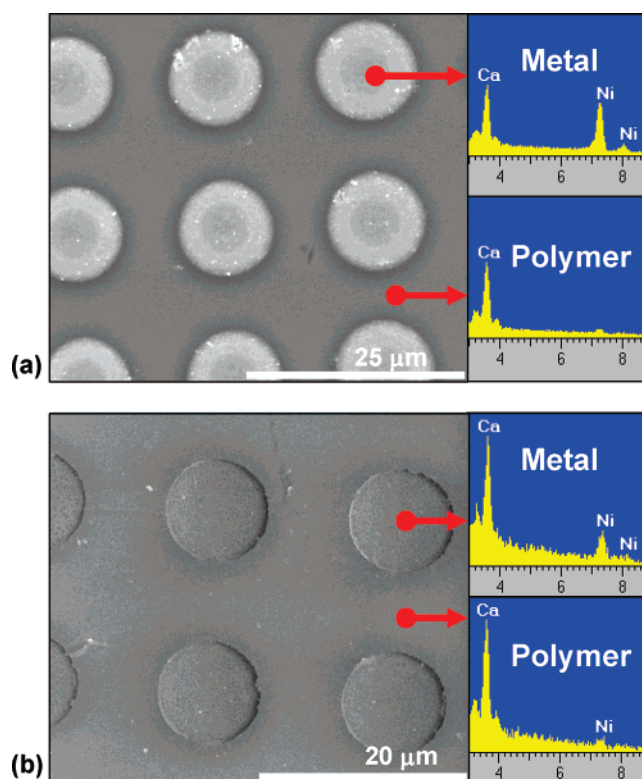


Figure 5. SEM images of patterned nickel samples created by methods 1 (a) and 2 (b). These images are accompanied with EDS spectra for the metal and polymer surfaces.

SEM was used to analyze the samples from methods 1 and 2 further because they are more appealing for practical applications. Figure 5 shows that the direct catalyst stamping method has a slightly better selectivity than the DA method. This is verified by the EDS spectra obtained for the two different samples. When the polymer spectra are compared with the nickel spectra of the same sample, the difference in the amount of nickel detected is much greater for method 1 than for method 2, so a larger difference in the nickel peaks means a larger difference in the amount of nickel deposited on the unpatterned regions.

The lower selectivity of method 2 as compared to that of method 1 suggests that the last layer of polyelectrolyte adsorbed is not the only layer that effects nickel deposition. The interpenetration of subsurface layers of polyelectrolyte may have an effect on the selectivity of the palladium ion and subsequent nickel deposition. Additionally, Decher and co-workers have shown that during the initial buildup of PEMs there exists a zone in which the substrate affects PEM formation.²⁵ This zone is ~ 4 bilayers in thickness. We investigated the effect of the number of bilayers on the patterning of nickel using method 2. Glass slides were coated with 0, 1, 3, and 5 bilayers of PDAC/SPS. These films have a thickness ranging from <5 to 18 nm.²⁶ Nickel patterns were then created using directed assembly. The resulting optical micrographs are shown in Figure 6. The images show that as the number of bilayers increases the selectivity and quality of the patterns increase. With only one bilayer, the quality of the patterns and the selectivity are low. With three bilayers, the selectivity is good; however, the patterning is still not complete. The five bilayer samples show an increase in the quality of the patterns. At more than five bilayers, the patterning quality and

(25) Ladam, G.; Schaad, P.; Voegel, J. C.; Schaaf, P.; Decher, G.; Cuisinier, F. *Langmuir* **2000**, *16*, 1249–1255.

(26) Clark, S. L.; Montague, M. F.; Hammond, P. T. *Macromolecules* **1997**, *30*, 7237–7244.

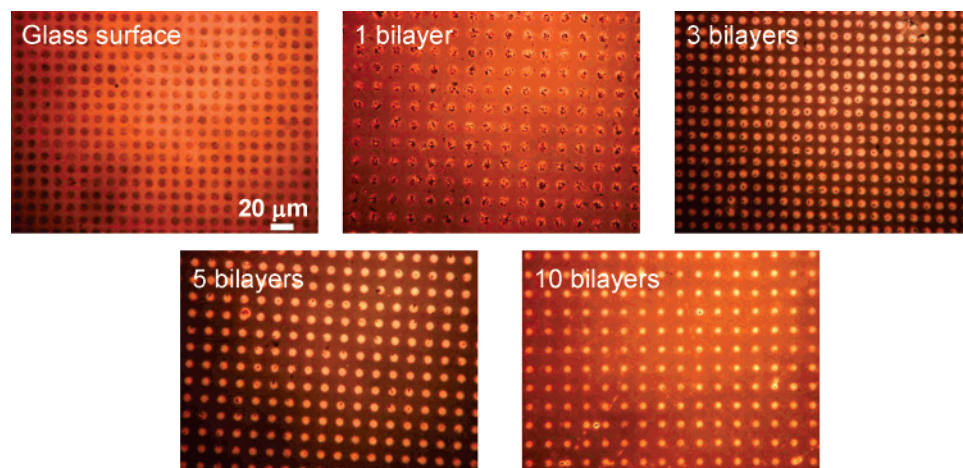


Figure 6. Optical microscope images of samples created using DA (method 2). The number of bilayers affects the selectivity and quality of the deposited nickel patterns. The scale bar is valid for all images.

selectivity have reached the same level as seen for the 10 bilayer slides that are normally used for method 2. Interestingly, when the negatively charged catalyst was exposed to the PAMAM patterned glass slide (0 PEM bilayers), the catalyst deposited preferentially onto the glass surface instead of the PAMAM dendrimers. We speculate this is due to the rapid hydrolysis of the palladium catalyst in solution and subsequent attachment to the $-OH$ -terminated surface at the low pH (~ 3) of our catalyst solution.^{27,28} The attachment of the hydrolysis product to the surface is not observed when the glass surface is coated with polyelectrolytes. Furthermore, at a pH of 3, the palladium complexes are competing with the protons to interact with the primary and tertiary amines of the PAMAM dendrimer. This causes the primary amines to become inert and the tertiary amines to react slowly to form covalent bonds with the palladium complexes.²² Because we use a 10 s immersion time, the palladium interacts only electrostatically with the dendrimers. Nickel deposition will occur as a result of these two processes. However, Figure 6 suggests that hydrolysis deposits more palladium onto the surface, which causes more nickel to be observed on the glass surface than in the PAMAM regions.

QCM was used to compare the plating rates of the three different catalyst introduction methods using a homogeneous surface. Gold-coated quartz crystals were coated with a $-COOH$ -terminated self-assembled monolayer (SAM). This SAM created a negatively charged surface that was then used as a starting point for PEM buildup. To simulate method 1, (PDAC/SPS)_{10.5} bilayer-coated crystals with an outer PDAC surface were catalyzed with palladium and placed in an electroless bath. Method 2 was simulated by starting with a (PDAC/SPS)₁₀ bilayer-coated crystal and adsorbing a layer of PAMAM dendrimers before the adsorption of the negatively charged catalyst. Additionally, a (PDAC/SPS)₁₀ bilayer-coated crystal was used to simulate the unpatterned SPS regions on the surface. Dendrimer-encapsulated nanoparticles were adsorbed onto the surface of a (PDAC/SPS)₁₀ bilayer-coated crystal to simulate method 3. The resulting kinetic data are shown in Figure 7. The nickel growth rate for all three methods has two general zones: an initial growth zone and then a linear growth zone. The plating rates for methods 1 (PDAC surface) and 2 (PAMAM surface) are virtually the same. However, method 3 (PAMAM and nanoparticle surface) has a slower initial

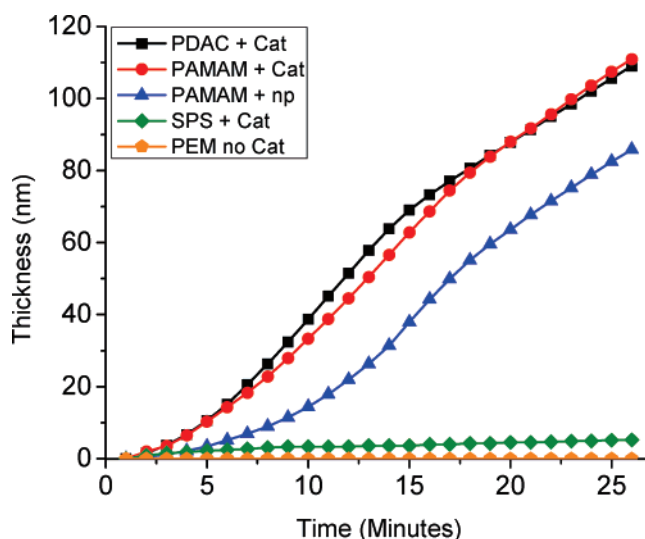


Figure 7. QCM data for homogeneous surfaces that represent the different regions on the patterned surfaces.

growth rate that requires a longer time before a linear growth rate is observed. This decrease in the initial growth rate is caused by the cage-like PAMAM dendrimers covering the surface of the palladium nanoparticle catalyst, which prevents nickel deposition from occurring as freely as in method 1 or 2. Once the surface is completely coated with metal, then a linear growth rate of ~ 4.7 nm/min is observed for all three methods. To confirm that a catalyst is required for electroless deposition, unpatterned surfaces of both SPS and PDAC were placed in an electroless bath. Neither surface type showed nickel plating (PEM with no catalyst). Negatively charged SPS surfaces catalyzed with the negative palladium catalyst showed a very small nickel growth rate. After 25 min, the nickel was only 4.6 nm thick. These data suggest that the interpenetration of PEMs allows for a small amount of catalyst to adsorb onto the outer SPS surface.

Conclusions

The methods used to introduce the catalyst to the PEM surfaces before electroless deposition significantly affected the nickel pattern selectivity and resulting morphology. Directly stamping the catalyst yielded the highest selectivity. Encapsulating the catalyst inside PAMAM dendrimers slowed the plating rate and caused an agglomerated morphology. DA created excellent metal patterns but did not have a high selectivity. The decreased

(27) Dressick, W. J.; Dulcey, C. S.; Georger, J. H.; Calabrese, G. S.; Calvert, J. M. *J. Electrochem. Soc.* **1994**, *141*, 210–220.

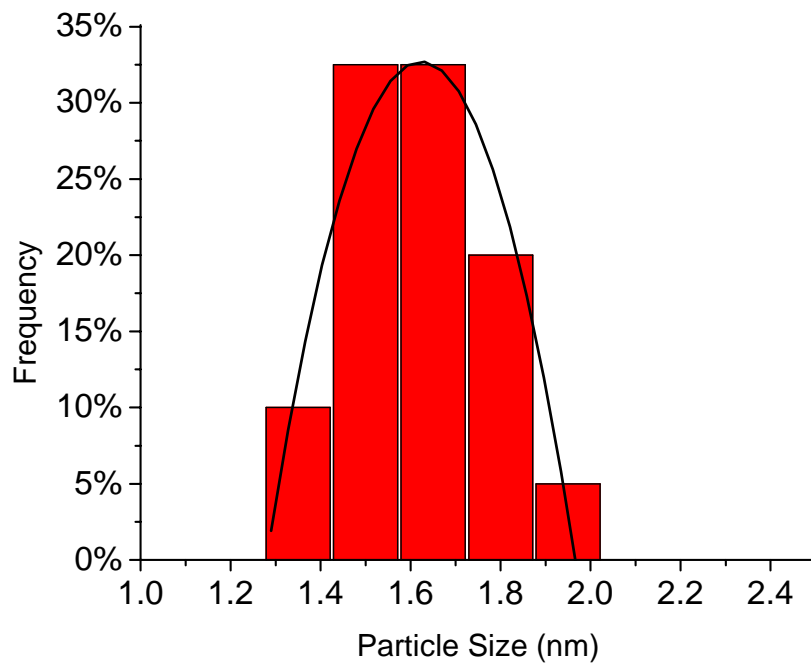
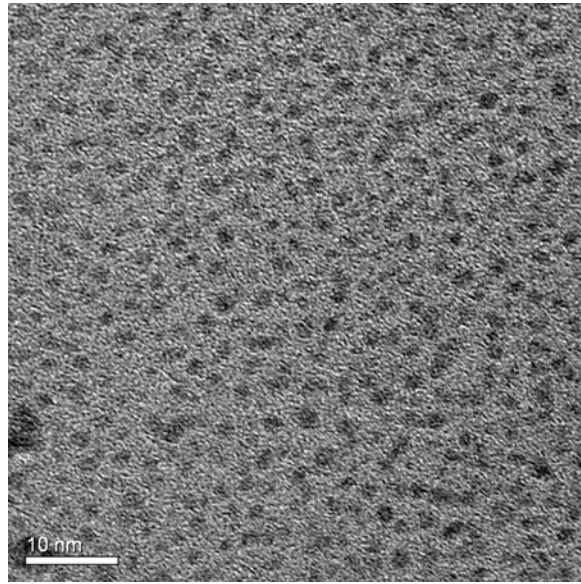
(28) Kind, H.; Bittner, A. M.; Cavalleri, O.; Kern, K.; Greber, T. *J. Phys. Chem. B* **1998**, *102*, 7582–7589.

selectivity was caused by the interpenetration of the subsurface PEM layers into the outer polyelectrolyte layer. The effect of the subsurface layers was also demonstrated when the substrate effect on electroless nickel deposition was removed by increasing the PEM film thickness. The nickel patterning was affected by the substrate until more than five polyelectrolyte bilayers were deposited on the surface. Our approach of combing PEM, μ CP, and ELD is versatile and inexpensive and allows for a wide variety of different substrates to be utilized. In addition, further modification of the surface is possible if additional functionality or the creation of bimetallic patterns is desired.

Acknowledgment. We thank the National Science Foundation (CTS-0609164), the AFOSR, the Michigan Economic Development Corporation, and the MSU Foundation for their funding of our project.

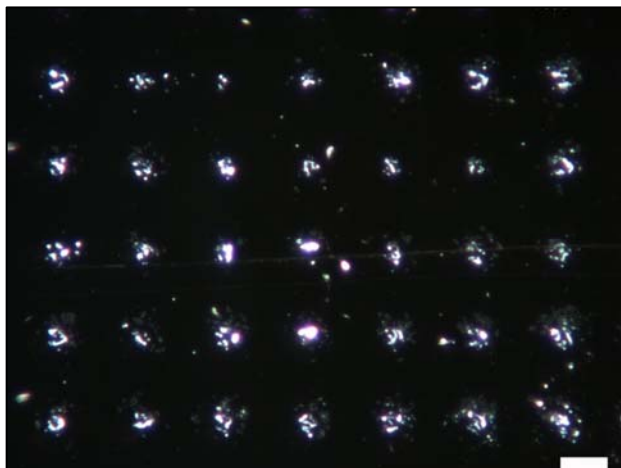
Supporting Information Available: Characterization of dendrimer-encapsulated palladium nanoparticles and an optical microscope image of patterned nickel deposition on dendrimer-encapsulated ions. This material is available free of charge via the Internet at <http://pubs.acs.org>.

LA7007232



(b)

SI 1: (a) TEM image of dendrimer encapsulated nanoparticles. (b) Chart of the nanoparticle size distribution.



SI 2: Dark-field optical microscope image of a sample that was created by stamping dendrimer encapsulated ions, followed by electroless deposition.